Atmos. Chem. Phys., 13, 4617–4630, 2013
www.atmos-chem-phys.net/13/4617/2013/
doi:10.5194/acp-13-4617-2013

Atmospheric Chemistry and Physics Open Access

On the export of reactive nitrogen from Asia: NO_x partitioning and effects on ozone

T. H. Bertram[1,*], A. E. Perring[1,], P. J. Wooldridge[1], J. Dibb[3], M. A. Avery[4], and R. C. Cohen[1,2]**

[1]Department of Chemistry, University of California, Berkeley, USA
[2]Department of Earth and Planetary Science, University of California, Berkeley, USA
[3]Institute for the Study of Earth, Oceans, and Space, University of New Hampshire, USA
[4]NASA Langley Research Center, Hampton, VA, USA
[*]now at: Department of Chemistry and Biochemistry, University of California, San Diego, USA
[**]now at: NOAA Earth System Research Laboratory, Boulder, CO, USA

Correspondence to: R. C. Cohen (rccohen@berkeley.edu)

Received: 4 September 2012 – Published in Atmos. Chem. Phys. Discuss.: 21 September 2012
Revised: 2 April 2013 – Accepted: 4 April 2013 – Published: 6 May 2013

Abstract. The partitioning of reactive nitrogen (NO_y) was measured over the remote North Pacific during spring 2006. Aircraft observations of NO, NO_2, total peroxy nitrates (ΣPNs), total alkyl and multi-functional nitrates (ΣANs) and nitric acid (HNO_3), made between 25° and 55° N, confirm a controlling role for peroxyacyl nitrates in NO_x production in aged Asian outflow. ΣPNs account for more than 60 % of NO_y above 5 km, while thermal dissociation limits their contribution to less than 10 % in the lower troposphere. Using simultaneous observations of NO_x, ΣPNs, ΣANs, HNO_3 and average wind speed, we calculate the flux of reactive nitrogen through the meridional plane of 150° W (between 20° and 55° N) to be 0.007 ± 0.002 Tg N day^{-1}, which provides an upper limit of 23 ± 6.5 % on the transport efficiency of NO_y from East Asia. Observations of NO_x, and HO_x are used to constrain a 0-D photochemical box model for the calculation of net photochemical ozone production or tendency (ΔO_3) as a function of aircraft altitude and NO_x concentrations. The model analysis indicates that the photochemical environment of the lower troposphere (altitude < 6 km) over the north Pacific is one of net O_3 destruction, with an experimentally determined crossover point between net O_3 destruction and net O_3 production of 60 pptv NO_x. Qualitative indicators of integrated net O_3 production derived from simultaneous measurements of O_3 and light alkanes (Parrish et al., 1992), also indicate that the north Pacific is, on average, a region of net O_3 destruction.

1 Introduction

The partitioning of reactive nitrogen (NO_y), among its various oxidation products, determines the spatial scales by which NO_x ($NO_x \equiv NO + NO_2$), or its temporary reservoirs, are transported. As a result, NO_y partitioning impacts the production rates of both ozone (O_3) and secondary organic and inorganic aerosol on local, regional and global scales. Analysis of trends in both O_3 concentration and reactive nitrogen on the west coast of North America indicate that background O_3 concentrations over the North Pacific have steadily risen over the past three decades (e.g., Jaffe et al., 2003; Parrish et al., 2009), with speculation that the growth in NO_x emission rates in eastern Asia is largely responsible (Richter et al., 2005; Zhang et al., 2007; Zhang et al., 2008; Zhang et al., 2009; Walker et al., 2010). The increase in background O_3 concentrations may limit the efficacy of future local and regional O_3 control strategies, particularly in California (Jacob et al., 1999; Cooper et al., 2010) although analysis of surface observations suggest most current violations in California are entirely under local control (Pusede and Cohen, 2012). Quantitative assessment of potential changes in the photochemistry of the North Pacific has been limited by a paucity of observation-based constraints. Using observations made primarily along the western coast of North America, Parrish et al. (2004a) concluded not only that background O_3 concentrations had increased over the past 2 decades by $\sim$10 ppbv, but that the trend in peroxyacetyl nitrate (PAN)

concentrations observed on the west coast of North America tracked the increase in NO_x emissions reported by Streets et al. (2003), and the net ozone production rate, or O_3 photochemical tendency ($\Delta(O_3)$) had slowed. Aircraft observations of O_3 and PAN concentrations and $\Delta(O_3)$ made in the eastern Pacific (east of 135° W, e.g., ITCT 2K2 and CITE-1C) have been compared with those made in the western Pacific (west of 155° E, e.g., PEM-WEST B and TRACE-P). However, there have been few tropospheric observations (outside of the transit flights for PEM-WEST B and TRACE-P that primarily sampled at the aircraft ceiling altitudes) that have sampled the remote Northern Pacific (between 155° E and 135° W). Here we discuss measurements made during the INTEX-B campaign aboard the NASA DC8 aircraft during April and May of 2006.

Prior to discussing the INTEX-B reactive nitrogen observations, we first briefly review NO_x oxidation mechanisms and highlight the aspects of the reaction mechanism that are of particular relevance in the North Pacific. During the daytime, NO_x can be sequestered from the catalytic O_3 production cycle following the three-body reaction of NO_2 with the hydroxyl radical (OH) to produce HNO_3 (Reaction R1), reaction with peroxy radicals (RO_2) to form a peroxy nitrate (RO_2NO_2) (Reaction R2), the most abundant being peroxy acetyl nitrate (or PAN) a derivative of acetaldehyde (Singh et al., 1985, 1986), or through the formation of alkyl or multi-functional nitrates ($RONO_2$) following the reaction of NO with RO_2 (Reaction R3) (Calvert and Madronich, 1987; Trainer et al., 1991).

$$NO_2 + OH + M \rightarrow HNO_3 + M \quad \text{(R1)}$$

$$NO_2 + RO_2 + M \leftrightarrow RO_2NO_2 + M \quad \text{(R2)}$$

$$NO + RO_2 + M \rightarrow RONO_2 + M \quad \text{(R3)}$$

NO_2 also reacts directly with O_3, producing the nitrate radical (NO_3), which quickly reaches thermodynamic equilibrium with dinitrogen pentoxide (N_2O_5) (Reactions R4–R5) (Noxon et al., 1978; Platt et al., 1980). NO_3 and N_2O_5 concentrations are limited during the day due to strong visible light absorption and subsequent dissociation of NO_3 as well as rapid reaction with NO (which is significantly reduced at night). Together these reactions limit the steady-state lifetime of NO_3 to seconds in sunlight.

$$NO_2 + O_3 \rightarrow NO_3 + O_2 \quad \text{(R4)}$$

$$NO_2 + NO_3 + M \leftrightarrow N_2O_5 + M \quad \text{(R5)}$$

Additionally, nitrous acid (HONO), formed through the hydrolysis of NO_2 has been shown to be a significant component of NO_y at night near the surface (Finlayson-Pitts et al., 2003).

The partitioning of reactive nitrogen between the various NO_x oxidation products is of great importance as each reservoir (e.g., RO_2NO_2, $RONO_2$, HNO_3 and N_2O_5) has a drastically different lifetime in the atmosphere. ΣPNs are largely insoluble (e.g., the Henry's Law Constant for PAN is 2–5 M atm^{-1} at 273 °K) (Sander, 1999), have low accommodation coefficients ($\gamma = 0.0001$) for heterogeneous uptake (Kirchner et al., 1990), and measurements have shown them to have small deposition velocities relative to other constituents of NO_y (Farmer et al., 2006; Turnipseed et al., 2006; Wolfe et al., 2009) leading to long atmospheric lifetimes that are limited by photolysis in the upper troposphere and thermal dissociation at warm temperatures characteristic of the lower troposphere. The PAN lifetime against thermal decomposition increases from hours to days in the BL to months in the UT where lower temperatures drive the equilibrium shown in Reaction (R2) to the right, toward RO_2NO_2 and photolysis limits the atmospheric lifetime to tens of days (Talukdar et al., 1995; Kirchner et al., 1999). As a result, ΣPNs that are formed in colder regions can be transported long distances in the free troposphere and serve as a net source of NO_x in warmer environments, far away from their source region (Lamarque et al., 1996; Moxim et al., 1996; Horowitz and Jacob, 1999; Heald et al., 2003; Hudman et al., 2004).

Nitric acid is largely soluble (e.g., the Henry's Law Constant for HNO_3 is $2–8 \times 10^5$ M atm^{-1} at 273 °K) (Sander, 1999), and has a significant accommodation coefficient for heterogeneous removal (Choi and Leu, 1998; Arora et al., 1999; Tolocka et al., 2002) and a large deposition velocity (Munger et al., 1996, 1998). Alkyl nitrates (ΣANs) are removed following photolysis or reaction with OH or O_3. In addition, hydroxyl- and multi-functional nitrates, which comprise a large fraction of ΣANs, especially in regions of strong biogenic influence (Day et al., 2003), are thought to be removed effectively via deposition and heterogeneous removal processes (Farmer et al., 2006). In the presence of high surface area loadings N_2O_5 can be hydrolyzed forming HNO_3 or $ClNO_2$ on chloride containing particles (Bertram and Thornton, 2009) and can be accommodated to the surface or dust particles (Tang et al., 2010), where the lifetime of $ClNO_2$ to photolysis is typically less than three hours. These chemical lifetimes and the associated partitioning among different NO_y species determine the extent to which NO_x is present in the atmosphere far from its source and, thus, have the potential to affect the rate of ozone production (e.g., Hudman, et al. 2004) and nitrogen deposition (e.g., Munger et al., 1996; Holland et al., 2005), downwind of the source region.

Previous aircraft observations of NO_y over the North Pacific indicate that NO_y is primarily comprised of PAN and HNO_3 (Koike et al., 1996; Singh et al., 1996; Talbot et al., 2003; Roberts et al., 2004). These measurements were confined closely to either the Asian or North American continents, with only a select number of transpacific flights that sampled the remote Pacific. The scientific objective of earlier flight campaigns was the characterisation of Asian outflow plumes near the source region (e.g., PEM West A, PEM West B and TRACE-P, Hoell et al., 1996, 1997; Jacob et al.,

2003). Transit flights from the United States to the sampling region proved instructive in assessing the extent of transport and transformation of the Asian plumes (Heald et al., 2003). Recently, the Intercontinental Transport and Chemical Transformation 2002 (ITCT 2K2) Experiment made observations of Asian plumes transported to North America during spring (Parrish et al., 2004b).

Observations of Fresh Asian Emissions: Measurements taken during the PEM West B campaign, indicated a major role for PAN (ranging between 20 and 70 % of NO_y) in Asian Outflow, and a NO_y budget that was closed to within the uncertainties of the measurements that comprise it (Singh et al., 1998). In these studies, Singh et al. described a strong latitudinal dependence in PAN, with NO_y sampled in the northern pacific having larger PAN fractions than in southern air. This was attributed to a strong gradient in temperature and, hence, PAN thermal dissociation. Talbot et al. (2003) showed from observations taken during the TRACE-P experiment that the PAN/NO_y ratio exhibited a strong vertical structure, again associated with the temperature dependence in the PAN thermal decomposition rate (Talbot et al., 2003).

Observations of Aged Asian Emissions: The aforementioned experiments were instructive in describing the partitioning of NO_y in the outflow region; however, they did little to address the question of long range transport of NO_y across the Pacific. To better address these questions, ITCT 2K2 was conducted in the Spring of 2002 to probe the chemical composition of Asian plumes that reach the North American Continent (Nowak et al., 2004). During these studies Roberts et al. measured a PAN to NO_y ratio, in transported Asian plumes, ranging between 0.5 and 0.7 in air-masses above 2 km and as large as 0.8 in episodic Asian plume events. The observed ratio dropped rapidly (to less than 0.2) at the surface, again consistent with the calculated PAN lifetime to thermal dissociation (Roberts et al., 2004). The PPN to PAN ratio in air transported from Asia, as measured on ITCT 2K2, was on average 0.12.

The dominance of PANs in aged Asian outflow was first discussed by Singh et al. (1986), and can be understood given the context for the export of pollution from Asia. The export of pollution from Asia is typically lofted via frontal lifting in warm conveyor belts or injected directly into the free troposphere via deep convection (Bey et al., 2001; Stohl, 2001; Liu et al., 2003). The exported pollution can then be transported across the Pacific on timescales of 5–10 days (Yienger et al., 2000; Jaffe et al., 2001), with peak outflow and transport occurring in the late spring (Yienger et al., 2000). Episodic events have been sampled in the continental United States (Jaffe et al., 1999, 2001) and their effect on air quality in the US has been the subject of many recent studies using large scale models (e.g., Fiore et al., 2002). The export process plays a critical role in the partitioning of NO_y at the point of injection into the free troposphere (Miyazaki et al., 2003). Due to wet removal of HNO_3 associated with both warm conveyor belt (WCB) lifting and deep convection and the short chemical lifetime of NO_x in the lower troposphere, NO_y is expected to be largely dominated by PAN in Asian outflow plumes sampled in the free troposphere. Since PAN is only thermally stable at altitudes greater than 2–6 km (depending on latitude), PAN is expected to be a large source of NO_x, and consequentially an O_3 precursor, in subsiding air-masses over the remote pacific (e.g., Jaffe et al., 1999; Kotchenruther et al., 2001a, b; Heald et al., 2003; Hudman et al., 2004; Zhang et al., 2008; Walker et al., 2010).

In what follows, we present observations of NO_2, ΣPNs, ΣANs, and HNO_3 made aboard the NASA DC-8 during the Intercontinental Chemical Transport Experiment – Phase B [INTEX-B] in April–May 2006 in the North Pacific (20–60° N, 175° E–135° W). We use these observations to: (1) provide constraint on the mass flux of reactive nitrogen through the North Pacific during spring, and (2) calculate both a quantitative instantaneous and a qualitative integrated net O_3 production rate (Parrish et al., 1992) that can be compared with previous observations made in both the eastern and western Pacific.

2 Experimental methods

2.1 Intercontinental chemical transport experiment – Phase B [INTEX-B]

We use observations obtained during the INTEX-B campaign, conducted out of Honolulu, HI and Anchorage, AK during April and May of 2006 using the NASA DC-8 (20–60° N, 175° E–135° W). Research flights were primarily conducted during daytime (88 % of the observations were made at SZA $< 90°$); the only nighttime flight was the transit between Honolulu and Anchorage. In the following analysis all observations were used. The principle objective of the INTEX-B campaign was to characterise the transport of Asian pollution, which is most frequent and rapid in spring, during periods of strong frontal activity (Yienger et al., 2000). Research flights were designed to sample pollution lofted from the Asian boundary layer (BL) by cold frontal activity and transported across the Pacific toward North America in the free troposphere. Observations highlighted in this study include in situ measurements of ozone, NO, NO_2, total peroxy nitrates (ΣPNs), total alkyl and multi-functional nitrates (ΣANs) and nitric acid (HNO_3) (Thornton et al., 2000; Day et al., 2002; Fairlie et al., 2007). Aircraft flight tracks are shown in Fig. 1a, where sampling legs north of 35° N are shown in black and sampling legs south of 35° N are shown in grey. The 35° N threshold was chosen as satellite observations and model analyses of enhancements in carbon monoxide, indicative of transpacific transport of Asian pollution, have shown strong influence north of 35° N (Zhang et al., 2008; Hsu et al., 2012) coinciding with the westward movement of air above the Pacific High. The corresponding mean vertical profile in temperature for the two sampling regions is

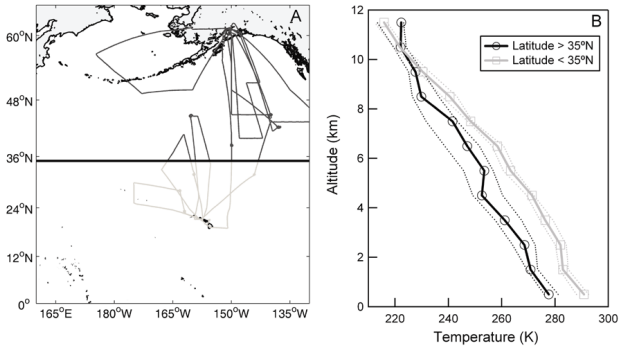

Fig. 1. (left panel) INTEX-B flight tracks made between 17 April 2006 and 15 May 2006 over the Northern Pacific Ocean. Sampling legs north of 35° N are shown in black, while legs south of 35° N are shown in grey. (right panel) Observed mean temperature within 1 km altitude bins between 0–12 km divided into Northern (black) and Southern (grey) sampling bins. The dashed lines represent one standard deviation of the mean.

shown in Fig. 1b, highlighting an approximately 10 °C difference in temperature between the two regions from the surface through the mid-troposphere. The implications of the observed temperature difference on the reactive nitrogen budget are discussed in detail in Sect. 3.2.

2.2 Instrument descriptions

Observations of NO_2, ΣPNs, ΣANs and HNO_3 were made using Thermal Dissociation – Laser Induced Fluorescence (TD-LIF) (Thornton et al., 2000; Day et al., 2002). Briefly, NO_2 fluorescence is detected following excitation of a specific jet-cooled rovibronic transition at 585 nm. The resulting fluorescence is collected by a PMT at 90° to the laser axis, which is both optically and temporally filtered to remove laser scatter. The measured fluorescence is directly correlated to NO_2 following calibration to a NIST traceable NO_2 calibration standard (accuracy of ±5 %) (Bertram et al., 2005). The NO_2 calibration constant was determined and applied as a function of inlet pressure due to the nonlinear response of the system to pressure, a result of reduced jet-cooling of NO_2 at low ambient pressures. Higher order reactive nitrogen classes (ΣPNs, ΣANs and HNO_3) are detected by coupling a thermal dissociation inlet to the LIF sensor (Day et al., 2002). In this system, we heat the ambient air stream to the dissociation threshold for the class of NO_y species of interest (200 °C for ΣPNs, 350 °C for ΣPNs +ΣANs, and 550 °C for ΣPNs + ΣANs + HNO_3) and detect the NO_2 dissociation product using NO_2 LIF. As configured for INTEX-B N_2O_5 would be detected in the ΣPNs channel (Fuchs et al., 2012), and $ClNO_2$ would likely be detected in the ΣANs channel based on the analysis of Thaler et al. (2011), however, this would likely only impact the nighttime transit flight and morning flights conducted before complete $ClNO_2$ photolysis. With regard to detection of particulate nitrate, unpublished laboratory measurements have shown that TD-LIF is sensitive to volatile particulate nitrate. The resulting NO_2, formed following the thermal dissociation of the precursor compound, would be detected in the corresponding TD-LIF channel (e.g., semi-volatile organic nitrate aerosols are detected as ΣANs). Specific discussion of alkylnitrates in the aerosol phase can be found in Rollins et al. (2012).

The TD-LIF instrument flown on INTEX-B consisted of two NO_2 LIF detection cells and four independent thermal dissociation ovens. The first detection cell alternated between sampling the ambient and 350 °C channel, and the second detection cell alternated between sampling the 200 °C and 550 °C channel. The sampling duty cycle was such that in each two minute sampling period, NO_2, ΣPNs, ΣANs, and HNO_3 were sampled for 90, 60, 15 and 15 s, respectively. The resulting system has an NO_2 detection limit of 8 pptv/10 s at 760 Torr (ground) and 25 pptv/10 s at 10 km at $S/N = 2$. The sensitivity of the TD-LIF technique toward ΣPNs, ΣANs and HNO_3 is determined by the partitioning of the individual components of NO_y as discussed in Day et al. (2002), Wooldridge et al. (2010) and Perring et al. (2010).

During the combined MILAGRO and INTEX-B flight campaigns, three wing-tip to wing-tip instrument comparison flights were conducted between the NASA DC-8 and NSF C-130 (Kleb et al., 2011). Direct comparisons for TD-LIF measurements of NO_2, ΣPNs, and HNO_3 were available. The details of the comparisons can be found in Kleb et al. (2011), alongside discussion of instrument precision, accuracy, and limit of detection. Comparison on chemiluminescence and LIF NO_2 measurements yielded a slope of 1.20 ± 0.01, intercept of -39.1 ± 1, and $R^2 = 0.87$, over a concentration range from the instruments limit of detection (LOD) to 796 pptv. Comparison on CIMS and TD-LIF ΣPNs measurements yielded a slope of 1.35 ± 0.03, intercept of -83 ± 10 and $R^2 = 0.94$, over a concentration range from the instruments LOD to 2175 pptv. Comparison on TD-LIF and mist chamber (also on DC-8) HNO_3 measurements yielded a slope of 0.91 ± 0.01, intercept of -28 ± 4, and $R^2 = 0.84$, over a concentration range from the instruments LOD to 7530 pptv. For the comparisons above, the technique is listed as x-axis (C-130) and y-axis (DC-8). No comparison was available for the TD-LIF ΣANs measurement, however, Beaver et al. (2012), demonstrate agreement between independent AN measurements made using CIMS and TD-LIF ΣANs measurements at the surface (BEARPEX 2009), $R^2 = 0.89$, slope 0.91.

In what follows, we also use collocated aircraft measurements of nitric oxide (NO), O_3, particulate nitrate (pNO_3^-), OH and HO_2, butane and ethane. Discussion of each measurement technique, along with its associated uncertainty can be found in Kleb et al. (2011).

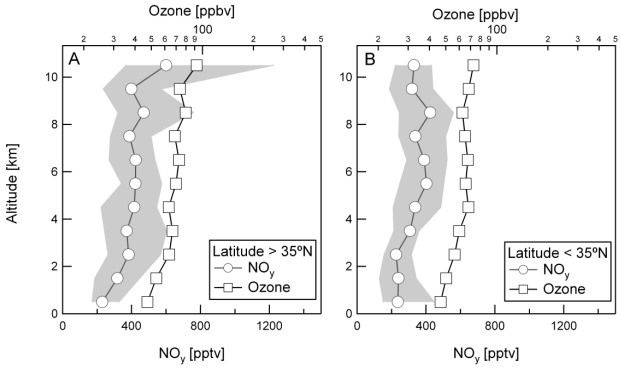

Fig. 2. Median vertical profile in ozone (black) and gas-phase NO_y (grey) ($NO_y \equiv NO_x + \Sigma PNs + \Sigma ANs + HNO_3$) as observed during the INTEX-B field campaign over the North Pacific during the Spring of 2006 (April–May), North of 35° N (left panel) and South of 35° N (right panel). The solid line depicts the median value in 1 km altitude bins and the shaded regions represent the interquartile range.

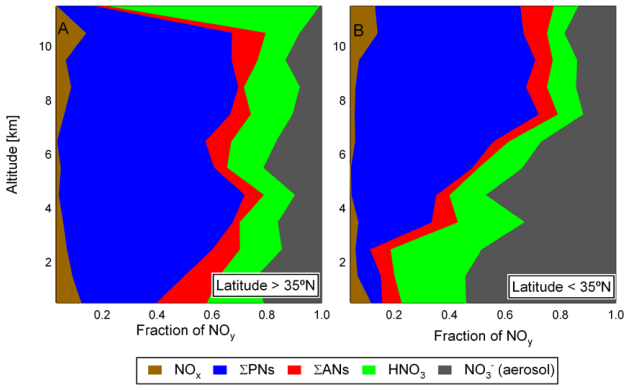

Fig. 3. Vertical distribution of the partitioning of reactive nitrogen (NO_y) between NO_x (brown), ΣPNs (blue), ΣANs (red), HNO_3 (green) and particulate nitrate (grey) as observed during the INTEX-B field campaign over the North Pacific during the Spring of 2006 (April–May), North of 35° N **(A)** and South of 35° N **(B)**. The fraction of NO_y in each altitude bin was calculated from the median profile in each of the individual constituents.

3 Results

3.1 Observations of reactive nitrogen during INTEX-B

The vertical distribution in the sum of the measured gas-phase components of NO_y (here defined as $NO_x + \Sigma PNs + \Sigma ANs + HNO_3$) are shown in Fig. 2, alongside the vertical profile in ozone for observations made both North (Fig. 2a) and South (Fig. 2a) of 35° N. Observations were separated into 1 km altitude bins, where the median in each bin is shown with a solid line, and the shaded region represents the interquartile range of the observations. The fraction of NO_y carried by particulate NO_3^- is not shown in Fig. 2, due to sparse data coverage, and limited sampling during vertical profiling. The contribution of particulate NO_3^-, as measured using mist chamber – ion chromatography (Talbot et al., 1997; Dibb et al., 2003), to the NO_y budget is shown in Fig. 3, and discussed below. The observed range in gas-phase NO_y mixing ratio (200–400 pptv) is broadly consistent with previous observations of NO_y in the both the eastern and western Pacific (Koike et al., 1996; Talbot et al., 2003; Nowak et al., 2004). Further, the vertical distribution of O_3 and NO_y are correlated in the troposphere reflecting their coupled source and sink mechanisms.

The partitioning of NO_y, between NO_x, ΣPNs, ΣANs, HNO_3, and aerosol nitrate is shown in Fig. 3 as a function of altitude. Here, the fraction of NO_y in each altitude bin was calculated from the mean profile of each of the individual constituents. In the upper troposphere (above 10 km), NO_y is largely composed of HNO_3, due to transport and mixing of stratospheric air, rich in HNO_3, to the upper troposphere and to the occasional sampling of purely stratospheric air in the northern pacific where the tropopause height (less than 10 km) is lower than the DC-8 aircraft ceiling (12.5 km). In the mid-troposphere (4–10 km) ΣPNs comprise as much as 80 % of total NO_y. In the lower troposphere (below 4 km), the ΣPN fraction again decreases, a result of the strong temperature dependence in the PAN thermal dissociation rate constant, where the instantaneous lifetime of PAN (at 35° N) goes from 20 days at 6 km to approximately two days at 4 km (Fig. 4). As a result, PAN thermal dissociation represents a significant source of NO_x to the remote troposphere. However, the NO_x lifetime with respect to reaction with OH is short, thus, NO_x produced by ΣPN decomposition is converted to HNO_3 on the time scale of days. The large fraction of HNO_3 in the lower troposphere is likely a result of the oxidation of NO_x, formed from the thermal dissociation of PAN in subsiding air-masses. While we cannot rule out the possibility of direct HNO_3 transport from the Asian continent to the sampling region such transport would appear to occur exclusively at low altitudes. In the upper troposphere, in the presence of mineral dust aerosol, gas-phase HNO_3 readily reacts heterogeneously with $CaCO_3$ resulting in the sequestration of nitrate in the particle phase as shown in Fig. 3 (Jordan et al., 2003; McNaughton et al., 2009).

3.2 Latitudinal gradients in ΣPNs

Latitudinal gradients in PAN have been observed previously in the lower troposphere (e.g., Singh et al., 1998; Roberts et al., 2004). This is due to the strong temperature dependence in the PAN thermal dissociation rate as shown in Fig. 4. At 2 km altitude, the instantaneous PAN lifetime increases from 0.2 days at 30° N to over 4 days at 50° N, at which point photolysis becomes the dominant loss process. The effect of PAN thermal dissociation is shown clearly in the vertical distribution of NO_y partitioning as a function of latitude. As shown

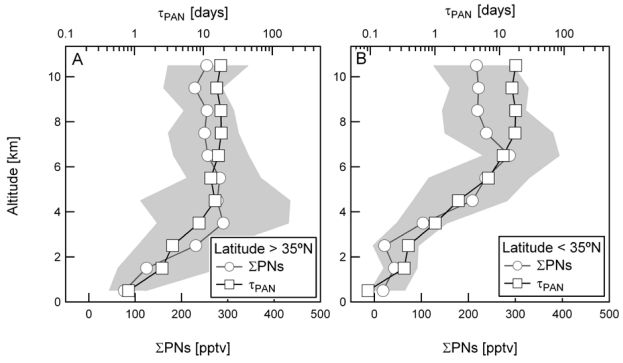

Fig. 4. Median vertical profile in ΣPNs (grey, -o-) and PAN instantaneous lifetime (τ_{PAN}) with respect to thermal dissociation, photolysis, and reaction with OH (black, -□-) as observed during the INTEX-B field campaign over the North Pacific during the Spring of 2006 (April–May), North of 35° N (left panel) and South of 35° N (right panel). The solid line depicts the median value in 1 km altitude bins and the shaded regions represent the interquartile range.

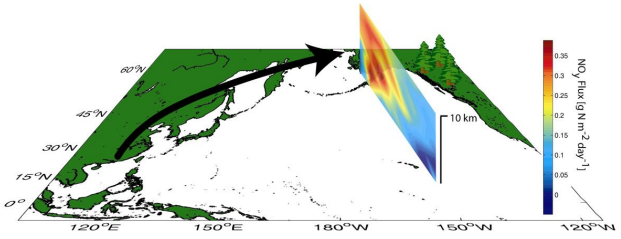

Fig. 5. Daytime flux of reactive nitrogen [gN m^2 day^{-1}] calculated using all available observations of gas-phase NO_y and wind-speed gridded into 5 latitude × 2 km altitude bins. Observations were filtered to remove strong stratospheric influence (O_3/CO > 1.25).

in Fig. 3, ΣPNs comprise over 40 % of NO_y from the surface to the tropopause north of 35° N. In contrast, southern samples (latitudes below 35° N) show a strong shift from the NO_y budget being controlled by ΣPNs to being dominated by the sum of HNO_3 and particulate NO_3^- at low altitudes, consistent with the profile shape of the PAN thermal dissociation rate.

4 Discussion

4.1 Intercontinental transport of reactive nitrogen

The extent to which the rapid increases in NO_x emissions, observed over East Asia during the past decade (Richter et al., 2005; Zhang et al., 2007), impact ozone production rates in the remote North Pacific and set the western boundary condition for North American regional air quality models is dependent on the chemical transformations that occur post emission and the export efficiency of NO_y from the source region to the free troposphere. NO_x emissions estimates over East Asia have been calculated using both top-down (Richter et al., 2005; Zhang et al., 2008; Walker et al., 2010) and bottom-up (Streets et al., 2003; Zhang et al., 2009) techniques. Due to rapid increases in NO_x emissions, we compare our observations with emission inventories that were calculated for the 2006 INTEX-B sampling period. Specifically, Zhang et al. (2009) estimated the total East Asian anthropogenic emissions of NO_x to be 11.2 Tg N yr^{-1} for 2006, where 6.3 Tg N yr^{-1} were attributed to anthropogenic emissions in China. Using a top-down approach, Zhang et al. (2008) calculated that the 2000 TRACE-P East Asian anthropogenic NO_x emissions inventory of Streets et al. (2003) (6.9 Tg N yr^{-1}) needed to be increased by nearly a factor of two to match 2006 OMI NO_2 observations.

The fraction of reactive nitrogen emissions that leave the boundary layer is dependent on both the transport mechanism and the partitioning of reactive nitrogen between its soluble and insoluble forms. Measurements made during the TRACE-P field campaign in 2000 indicated that the time averaged export flux of NO_y across the 130° E meridonial plane between 30° and 40° N was 8 % between 0 and 2 km and 10 % between 2 and 7 km (Koike et al., 2003). The measurements of Koike et al. indicate that a total of 18 % of emitted NO_y is transported out of the source region.

During INTEX-B, the DC-8 sampled between 20–60° N in the region of 175° E–135° W (Fig. 1a). This sampling domain is characterised by zonal flow from Asia to North America with higher wind speeds recorded at higher altitudes and in the Northern section of the sampling domain (Hudman et al., 2004). Forster et al. (2004) calculated a 15 yr climatology for the average transport of Asian CO for the months of March, April, and May. As shown in Fig. 2b of Forster et al. (2004), the Asian CO tracer is concentrated between 20–50° N (but extends all the way to 80° N) and 3–12 km at 125° W. For the INTEX-B sampling period, Walker et al. (2010) and Zhang et al. (2008), using satellite observations of CO and O_3 in combination with kinematic back trajectory analysis, show that transpacific transport of Asian pollution during this INTEX-B sampling period was found to be North of 20° N at 150° W.

To calculate the flux of nitrogen across the North Pacific between 20° and 55° N, we first construct curtain plots from the mean values of the westerly component of the observed wind speed and gas-phase NO_y number density binned into 2 km altitude and 5° latitude bins. For each of the sampling bins considered here, average westerly component of the wind speed and NO_y number density were uncorrelated ($R^2 < 0.2$). We then calculate the flux as the product of these two observable properties (Fig. 5). The total daytime flux through this window for the INTEX-B sampling period is 0.007 ± 0.002 Tg N day^{-1}. The observed gas-phase NO_y flux is 10 % NO_x, 62 % total peroxyacyl nitrates, 5 % alkyl

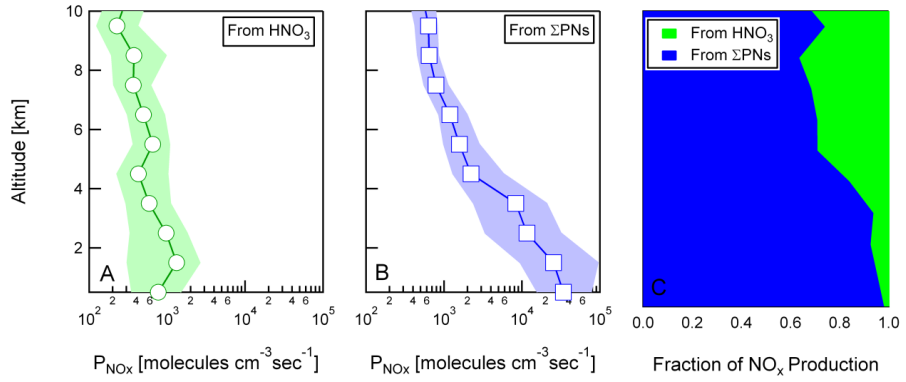

Fig. 6. Diurnally averaged NO_X production rates (molecules cm^{-3} s^{-1}) from nitric acid (left) and ΣPNs (centre) as a function of altitude. The fraction of NO_X production from each channel is shown in the right panel. Observations were filtered to remove strong stratospheric influence (O_3/CO > 1.25) and are for the northern pacific (Latitude > 35° N).

nitrates and approximately 23 % nitric acid. Particulate nitrate was not included in the above analysis due to sparse data coverage, based on the altitude and latitude range where the flux is largest and the percent of NO_y in the form of pNO_3, we expect that the contribution of pNO_3 (not accounted for here) to the daytime flux to be to be of order 10 %.

If we assume that all transpacific transport of Asian pollution crossing the 150° W meridonial plane proceeds through the 20–55° N sampling window, we can compare the magnitude of the observed gas-phase NO_y flux with the NO_x emissions inventories for East Asia to provide an estimate on the fraction of NO_x emissions that pass through the North Pacific en route to North America. Using the Zhang et al. (2009) bottom up inventory for East Asia anthropogenic NO_x emissions (11.2 Tg N yr^{-1}), our observation represents an upper limit of 23 ± 6.5 % for the fraction of Asian NO_x emissions that pass through the North Pacific (20–55° N).

The sample calculation has three important caveats: (1) as discussed in Forster et al. (2004), a small fraction of transpacific transport is carried north of the sampling window discussed here. (2) the above calculation represents an upper limit as the observed NO_y is also impacted by other sources such as biomass burning and stratospheric exchange, and (3) transpacific transport of Asian pollution is known to be episodic. Due to limited sample coverage, it was not possible to conduct this analysis with shorter time resolution. As discussed in Walker et al. (2010) and Zhang et al. (2008), a transport event was observed between 5–9 May 2006, which the DC-8 sampled on several occasions.

4.2 NO_x production rates

To investigate the chemical and thermal repartitioning of NO_y in the INTEX-B sampling region, we calculate the diurnally averaged, altitude dependent NO_x production rates (molecules cm^{-3} s^{-1}) from the thermal decomposition of ΣPNs and the photolysis and reaction of hydroxyl radicals with HNO_3 using our ambient observations coupled with the aforementioned time-dependent chemical box-model. As shown in Fig. 6, the fraction of NO_x produced from ΣPNs is strongly altitude dependent, reflecting both the temperature dependence in the thermal decomposition rate and the concentration profile shown in Fig. 4. As a result, NO_x production from HNO_3 becomes an increasing fraction of the total production rate with increasing altitude, accounting for nearly 30 % of in situ NO_x production above 5 km. This further highlights the importance of accurate representation of HNO_3 in chemical transport models.

4.3 Photochemical ozone production

The production rate of O_3 in the troposphere is primarily controlled by the cycling of NO_x in the presence of volatile organic carbon (VOC), oxidants and sunlight. In order to accurately model current O_3 abundances and assess the impact of future control strategies, it is critical to attain a mechanistic understanding of the chemical processes that drive O_3 production in the troposphere. In what follows, we investigate O_3 photochemical production in the North Pacific using two separate approaches: (1) quantitative calculation of the net instantaneous ozone production rate (ΔO_3), and (2) qualitative assessment of the integrated ΔO_3 using observations of O_3 and ratios of hydrocarbons (Parrish et al., 1992).

We calculate the instantaneous net O_3 production rate (ΔO_3) directly from measurements of NO (chemiluminescence), NO_2 (LIF; Thornton et al., 2000), OH and HO_2 (LIF; Faloona et al., 2004), H_2O (Diode laser hygrometer; Diskin et al., 2002), and O_3 (chemiluminescence; Fairlie et al., 2007), and calculations of $O(^1D)$ and RO_2 made using a photochemical box model constrained by observations of C1–C5 straight chain hydrocarbons using Eqs. (1–3) (Thornton et al., 2002).

$$\Delta_{O_x} = P_{O_x} - L_{O_x} \quad (1)$$

$$P_{O_x} = k_{NO+HO_2}[NO][HO_2] + \sum_i k_{NO+RO_2(i)}[NO][RO_2(i)] \quad (2)$$

$$L_{O_x} = k_{OH+NO_2+M}[M][NO_2][OH] + k_{O(^1D)+H_2O}\left[O\left(^1D\right)\right][H_2O] + k_{HO_2+O_3}[O_3][HO_2] + k_{OH+O_3}[O_3][OH] \quad (3)$$

The uncertainty in ΔO_3 can be large, especially at low NO_x concentrations ($[NO_x] < 100$ pptv) observed over the North Pacific. Specifically, systematic error in the measurement of NO and NO_2 have the potential to bias the calculation significantly. Comparison of the observed NO_2/NO ratio with that calculated from steady-state (Eq. 4) is a useful test of the validity of the measurements at low NO_x concentrations. Figure 7b shows the ratio of the observed NO/NO_2 ratio to that calculated via PSS from measurements of O_3, HO_2 and $J(NO_2)$ and model calculations of RO_2 as a function of measured NO_x. The results suggest that systematic error in the measurement of NO or NO_2 may be important at NO_x concentrations below 20 ppt, where the ratio of the observations to model calculations is 0.46. This is likely either a systematic positive bias in NO or negative bias in NO_2, both of which would result in a systematic over estimate of ΔO_3 for $NO_x < 20$ pptv (~ 20 % of the data).

$$\frac{NO_2}{NO} = \frac{k_{NO+O_3}[O_3] + k_{NO+HO_2}[HO_2] + \sum_i k_{NO+RO_2(i)}[RO_2(i)]}{J_{NO_2}} \quad (4)$$

The dependence of ΔO_3 on NO_x is shown in Fig. 7c, where ΔO_3 is calculated from atmospheric measurements of the components defined in Eqs. (1–3), for all INTEX-B samples where the PAN lifetime was less than ten days. The frequency distribution of NO_x mixing ratio is shown in Fig. 7a. While this analysis averages over a wide variety of chemical environments and VOC reactivity, it is instructive in describing the mean behaviour of the lower troposphere over the remote pacific and its sensitivity to increasing NO_x loadings.

The altitude dependence of both the instantaneous and diel averaged ΔO_3 are shown in Table 1, alongside previous model determinations of ΔO_3 in both the eastern and western Pacific. During INTEX-B, 24 h averaged mean ΔO_3 were calculated to be -0.12 ± 0.16, -0.05 ± 0.14, -0.02 ± 0.10 for 0–2 km, 2–4 km, and 4–6 km, respectively. Instantaneous mean ΔO_3 were calculated to be -1.13 ± 1.53, -0.47 ± 1.29, -0.14 ± 1.04 for 0–2 km, 2–4 km, and 4–6 km, respectively. The stated uncertainty in ΔO_3 is 1σ, and reflects a combination of atmospheric variability and instrument uncertainty. The increase in ΔO_3 with altitude is driven primarily by a decrease in $[H_2O]$ resulting in a corresponding decrease in $L(O_3)$. The diel averaged calculations indicate that on average, the photochemical environment below 6 km in the North Pacific is one of net O_3 destruction.

The average instantaneous ΔO_3 is statistically lower for INTEX-B (2006) than the corresponding measurements of ΔO_3 made during CITE-1C (1984) in the eastern Pacific,

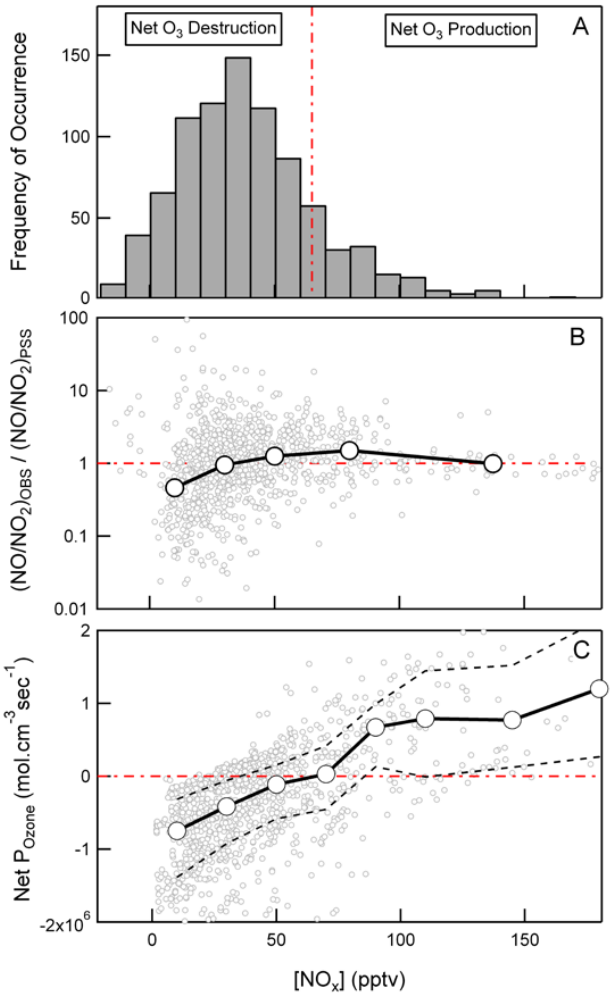

Fig. 7. (A) Observed frequency distribution of NO_x below 6 km. **(B)** Ratio of the observed NO_2/NO, compared with that calculated from photo-stationary steady state (Eq. 4). **(C)** Calculated instantaneous net ozone production rate as a function of observed NO_x concentrations. Observations were filtered to strongly remove stratospheric influence (O_3/CO > 1.25) and are for the northern pacific sampling region (Latitude > 35° N).

potentially reflecting a shift in hydrocarbon concentrations and/or oxidant loadings (Chameides et al., 1989). However, more likely the differences in ΔO_3 reflect the measured factor of two enhancement in NO between CITE-1C and INTEX-B (Table 1). The altitude dependent, diel averaged ΔO_3 compares well with that determined during PHOBEA (-0.83, -0.34 and -0.24), at comparable NO concentrations (Kotchenruther et al., 2001c). For comparison, ΔO_3 calculated for the PEM-WEST B and TRACE-P campaigns in the western Pacific reflects a net O_3 production regime (Crawford et al., 1997; Davis et al., 2003). This is presumed to be driven by statistically higher concentrations of NO_x (as much as a factor of three).

Table 1. Model calculated net ozone production rates (ΔO_3), constrained by aircraft observations made in the troposphere over the Eastern, Central and Western North Pacific.

Study, Location	Time Periods	Altitude (km)	NO, NO_x (pptv)	ΔO_3 (24 h average, instantaneous)[2,3]	Reference
CITE-1C 24–35° N 124–135° W	9 May 1984 [Flight 10]	0–2 2–4 4–6.4	(5, NR)[4] (8, NR)[4] (7, NR)[4]	(NR, −0.7) (NR, −0.37) (NR, −0.1)	Chameides et al. (1989)
PHOBEA 39–48° N 125–129° W	March–April 1999	0–2 2–4 4–6	(9.5, 31.4)[5,6] (12.4, 33.4)[5,6] (13.5, 45.6)[5,6]	(−0.83, NR) (−0.34, NR) (−0.24, NR)	Kotchenruther et al. (2001)
PEM-WEST B 25–45° N 120–155° E	February–March 1994	0–1 1–4	(30, NR)[7] NR	(1.28, NR)[7] (0.99, NR)[7]	Davis et al. (2003), Crawford et al. (1997)
TRACE – P 25–45° N 120–155° E	March–April 2001	0–1 1–4	(44, NR)[7] NR	(3.14, NR)[7] (0.69, NR)[7]	Davis et al. (2003)
INTEX-B 20–62° N 175° E– 135° W	April–May 2006	0–2 2–4 4–6	$(10 \pm 7, 24 \pm 23)$ $(12 \pm 9, 33 \pm 25)$ $(13 \pm 10, 26 \pm 24)$	$(-1.13 \pm 1.53, -0.12 \pm 0.16)$ $(-0.47 \pm 1.29 -0.05 \pm 0.14)$ $(-0.14 \pm 1.04, -0.02 \pm 0.10)$	this study

[1] NR = Not Reported.
[2] Units for 24 h average ΔO_3 are ppbv d^{-1}.
[3] Units for instantaneous ΔO_3 are ppbv h^{-1}.
[4] NO measurement for CITE-2 is taken from the Wallops NO chemiluminescence instrument.
[5] NO_x concentrations for PHOBEA include NO, NO_2, NO_3, HNO_4, HONO, 2 N_2O_5.
[6] [NO] for PHOBEA is estimated as NO_x-NO_2-HNO_4.
[7] NO and ΔO_3 measurements for PEM-WEST B and TRACE-P are binned medians.
[8] Reported uncertainty for INTEX-B measurements is 1σ.

To investigate the dependence of O_3 production on NO_x concentration, we calculate ΔO_3 as a function of NO_x where τ_{PAN} is less than 10 days. As shown in Fig. 7c, ΔO_3 increases linearly with increasing NO_x, exhibiting NO_x-limited behaviour over the entire sampling regime. In this low NO_x regime, the crossover point between net O_3 destruction and net O_3 production, has been identified at around 60 pptv, consistent with the early work of Fishman et al. (1979) as well as the analyses presented above. This key diagnostic is critical for assessing how future increases in NO_x emissions will affect global O_3 abundances and illustrates the sensitivity of the global O_3 budget to increasing NO_x. As a result, quantifying the magnitude and spatiotemporal distribution of NO_x and its transport and chemical evolution is crucial for modelling of tropospheric O_3.

One limitation of the aforementioned model calculation of ΔO_3 is that it provides a measure of the instantaneous ozone production rate under a specific set of conditions, making it difficult to determine the total ozone produced since emission without detailed knowledge of the time history of NO_x. Here, we follow the approach of Parrish et al. (1992, 2004a), and examine the correlation between O_3 and the natural log of the propane to ethane ratio. As shown in Fig. 8, the positive slope indicates that the photochemical environment of the north Pacific is still one of net O_3 destruction (for air masses sampled between 0–1 and 1–2 km). The magnitude of the slope has been used previously to provide a qualitative assessment of changes in the photochemical environment over the north Pacific (Parrish et al., 2004a). Specifically, the less negative slope (0.19 ± 0.06) measured during ITCT 2K2 (2002) as compared with that determined in 1985 at Pt. Arena, CA (0.86 ± 0.1) was interpreted as a decrease in the efficiency of photochemical O_3 destruction (Table 2). Interpretation of the observations within the context of the Parrish et al. (2004a) analysis would indicate that the photochemical environment became more efficient at O_3 destruction between 2002 and 2006. This interpretation would be inconsistent with the measured trend in NO_x emissions in eastern Asia between 2002 and 2006 (Zhang et al., 2009). Another interpretation would be that the difference between the slopes calculated for the ITCT 2K2 and INTEX-B campaigns reflects a difference in the altitude of the air mass trajectory

Table 2. Qualitative determinations of integrated net ozone production rates as determined from correlations between ozone and the ratio of propane to ethane.

Study, Location	Time Periods	Altitude (km)	$\ln(O_3)$/ ln(propane/ ethane)*	r	Reference
ITCT-2K2 30–40° N 105–135° W	April–May 2002	0–2	0.19 ± 0.06	0.49	Parrish et al. (2004)
Pt. Arena, CA 38°57′ N 123°44′ W	April–May 1985	20 m	0.86 ± 0.10	0.86	Parrish et al. (2004)
Cheeka Peak, 48°18′ N, 124°36′ W	1997–2002	480 m	-0.03 ± 0.08	−0.12	Parrish et al. (2004)
PHOBEA 39–48° N 125–129° W		0–2			
PEM-WEST B 25–45° N 120–155° E	February–March 1994	0–1	-0.39 ± 0.11	−0.55	Parrish et al. (2004)
TRACE – P 25–45° N 120–155° E	March–April 2001	0–1	0.19 ± 0.04	0.37	Parrish et al. (2004)
INTEX-B 20–62° N 175° E– 135° W	April–May 2006	0–1 1–2	0.46 ± 0.02 0.54 ± 0.04	0.78 0.78	this study

* Ratio reported is the slope of the linear least squares fit to the correlation between the natural log in O_3 with the natural log of the propane-to-ethane ratio (as shown in Fig. 6 for the INTEX-B data). The error represents the 95 % confidence limit.

from the source region to the sampling region and or the degree to which background or stratospheric air is entrained into the sampled air mass.

5 Conclusions

The observations presented here provide experimental measures of the partitioning of reactive nitrogen in the remote Pacific and provide an opportunity to test model representations of the transport and chemical evolution of NO_y from the Asian continent. In agreement with previous studies, we find a dominant role for ΣPNs throughout the Pacific region, displaying a strong latitudinal dependence, consistent with the known temperature dependence in the thermal dissociation of PAN. Using simultaneous observations of NO_x, ΣPNs, ΣANs, HNO_3 and average wind speed, we calculate the flux of reactive nitrogen through the meridional plane of 150° W (between 20° and 55° N) to be 0.007 ± 0.002 Tg N day^{-1}, which provides an upper limit of 23 ± 6.5 % on the transport efficiency of NO_y from East Asia. Observations of NO_x, and HO_x are used to constrain a 0-D photochemical box

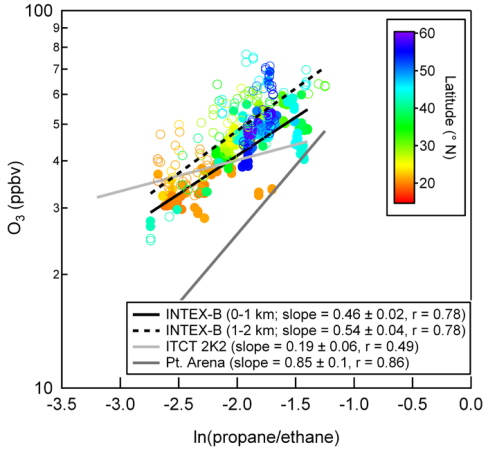

Fig. 8. Correlation of the measured O_3 concentrations with the natural log of the propane to ethane ratio in the marine boundary layer during INTEX-B. Linear least squares fits determined using data from ITCT 2K2 and Pt. Arena, CA are included for comparison Parrish et al. (2004).

model for the calculation of net photochemical ozone production or tendency (ΔO_3) as a function of aircraft altitude and NO_x concentrations. The model analysis indicates that the photochemical environment of the lower troposphere (altitude < 6 km) over the north Pacific is one of net O_3 destruction. Qualitative indicators of integrated net O_3 production derived from simultaneous measurements of O_3 and light alkanes (Parrish et al., 1992), also indicate that the north Pacific is on average net O_3 destruction, however, comparison with previous analyses suggests that interpretation of the trend in the correlation between O_3 and the ratio of propane to ethane requires careful assessment of air mass trajectory and entrainment of background and/or stratospheric air.

Acknowledgements. The authors thank the flight and ground crews of the NASA DC-8 Aircraft and the entire INTEX-B science team for their contributions during the 2006 intensive field campaign. We acknowledge Glen Sachse, Glenn Diskin, Greg Huey, Bill Brune, Jim Crawford, and Daniel Jacob for contributed data and/or model results. Work at U.C. Berkeley was supported under NASA grants NNX08AE56G, NNG05GH196, and NAG5-13668. The INTEX-B field programme was supported by the NASA-ESE Tropospheric Chemistry Programme. AEP acknowledges the NASA ESSF Programme.

Edited by: R. McLaren

References

Arora, O. P., Cziczo, D. J., Morgan, A. M., Abbott, J. P. D., and Niedziela, R. F.: Uptake of nitric acid by sub-micron-sized ice particles, Geophys. Res. Lett., 26, 3621–3624, 1999.

Beaver, M. R., Clair, J. M. St., Paulot, F., Spencer, K. M., Crounse, J. D., LaFranchi, B. W., Min, K. E., Pusede, S. E., Wooldridge, P. J., Schade, G. W., Park, C., Cohen, R. C., and Wennberg, P. O.: Importance of biogenic precursors to the budget of organic nitrates: observations of multi-functional organic nitrates by CIMS and TD-LIF during BEARPEX 2009, Atmos. Chem. Phys., 12, 5773–5785, doi:10.5194/acp-12-5773-2012, 2012.

Bertram, T. H. and Thornton, J. A.: Toward a general parameterization of N_2O_5 reactivity on aqueous particles: the competing effects of particle liquid water, nitrate and chloride, Atmos. Chem. Phys., 9, 8351–8363, doi:10.5194/acp-9-8351-2009, 2009.

Bertram, T. H., Cohen, R. C., Thorn, W. J., and Chu, P. M.: Consistency of ozone and nitrogen oxides standards at tropospherically relevant mixing ratios, J. Air Waste Manage., 55, 1473–1479, 2005.

Bey, I., Jacob, D. J., Logan, J. A., and Yantosca, R. M.: Asian chemical outflow to the Pacific in spring: Origins, pathways, and budgets, J. Geophys. Res., 106, 23097–23113, 2001.

Calvert, J. G. and Madronich, S.: Theoretical study of the initial products of the atmospheric oxidation of hydrocarbons, J. Geophys. Res.-Atmos., 92, 2211–2220, 1987.

Chameides, W. L., Davis, D. D., Gregory, G. L., Sachse, G., and Torres, A. L.: Ozone precursors and ozone photochemistry over eastern North Pacific during the spring of 1984 based on the NASA GTE CITE-1 airborne observations, J. Geophys. Res.-Atmos., 94, 9799–9808, 1989.

Choi, W. and Leu, M. T.: Nitric acid uptake and decomposition on black carbon (soot) surfaces: Its implications for the upper troposphere and lower stratosphere, J. Phys. Chem. A, 102, 7618–7630, 1998.

Cooper, O. R., Parrish, D. D., Stohl, A., Trainer, M., Nedelec, P., Thouret, V., Cammas, J. P., Oltmans, S. J., Johnson, B. J., Tarasick, D., Leblanc, T., McDermid, I. S., Jaffe, D., Gao, R., Stith, J., Ryerson, T., Aikin, K., Campos, T., Weinheimer, A., and Avery, M. A.: Increasing springtime ozone mixing ratios in the free troposphere over western North America, Nature, 463, 344–348, doi:10.1038/Nature08708, 2010.

Crawford, J. H., Davis, D. D., Chen, G., Bradshaw, J., Sandholm, S., Kondo, Y., Merrill, J., Liu, S., Browell, E., Gregory, G., Anderson, B., Sachse, G., Barrick, J., Blake, D., Talbot, R., and Pueschel, R.: Implications of large scale shifts in tropospheric NO_x levels in the remote tropical Pacific, J. Geophys. Res.-Atmos., 102, 28447–28468, 1997.

Davis, D. D., Chen, G., Crawford, J. H., Liu, S., Tan, D., Sandholm, S. T., Jing, P., Cunnold, D. M., DiNunno, B., Browell, E. V., Grant, W. B., Fenn, M. A., Anderson, B. E., Barrick, J. D., Sachse, G. W., Vay, S. A., Hudgins, C. H., Avery, M. A., Lefer, B., Shetter, R. E., Heikes, B. G., Blake, D. R., Blake, N., Kondo, Y., and Oltmans, S.: An assessment of western North Pacific ozone photochemistry based on springtime observations from NASA's PEM-West B (1994) and TRACE-P (2001) field studies, J. Geophys. Res.-Atmos., 108, 8829, doi:10.1029/2002JD003232, 2003.

Day, D. A., Wooldridge, P. J., Dillon, M. B., Thornton, J. A., and Cohen, R. C.: A thermal dissociation laser-induced fluorescence instrument for in situ detection of NO_2, peroxy nitrates, alkyl nitrates, and HNO_3, J. Geophys. Res.-Atmos., 107, 4046, doi:10.1029/2001JD000779, 2002.

Day, D. A., Dillon, M. B., Wooldridge, P. J., Thornton, J. A., Rosen, R. S., Wood, E. C., and Cohen, R. C.: On alkyl nitrates, O_3, and the "missing NO_y", J. Geophys. Res.-Atmos, 108, 4501, doi:10.1029/2003JD003685, 2003.

Dibb, J. E., Talbot, R. W., Scheuer, E. M., Seid, G., Avery, M. A., and Singh, H. B.: Aerosol chemical composition in Asian continental outflow during the TRACE-P campaign: Comparison with PEM-West B, J. Geophys. Res.-Atmos., 108, 8815, doi:10.1029/2002JD003111, 2003.

Diskin, G. S., Podolske, J., Sachse, G., and Slate, T.: Open-path airborne tunable diode laser hygrometer, Proc. SPIE, 4817, 2002.

Fairlie, T. D., Avery, M. A., Pierce, R. B., Al-Saadi, J., Dibb, J., and Sachse, G.: Impact of multiscale dynamical processes and mixing on the chemical composition of the upper troposphere and lower stratosphere during the Intercontinental Chemical Transport Experiment-North America, J. Geophys. Res.-Atmos., 112, D16s90, doi:10.1029/2006JD007923, 2007.

Faloona, I. C., Tan, D., Lesher, R. L., Hazen, N. L., Frame, C. L., Simpas, J. B., Harder, H., Martinez, M., Di Carlo, P., Ren, X. R., and Brune, W. H.: A laser-induced fluorescence instrument for detecting tropospheric OH and HO_2: Characteristics and calibration, J. Atmos. Chem., 47, 139–167, 2004.

Farmer, D. K., Wooldridge, P. J., and Cohen, R. C.: Application of thermal-dissociation laser induced fluorescence (TD-LIF) to measurement of HNO_3, Salkyl nitrates, Speroxy nitrates, and

NO_2 fluxes using eddy covariance, Atmos. Chem. Phys., 6, 3471–3486, doi:10.5194/acp-6-3471-2006, 2006.

Finlayson-Pitts, B. J., Wingen, L. M., Sumner, A. L., Syomin, D., and Ramazan, K. A.: The heterogeneous hydrolysis of NO_2 in laboratory systems and in outdoor and indoor atmospheres: An integrated mechanism, Phys. Chem. Chem. Phys., 5, 223–242, doi:10.1039/B208564J, 2003.

Fiore, A. M., Jacob, D. J., Bey, I., Yantosca, R. M. , Field, B. D., Fusco, A. C., and Wilkinson, J. G.: Background ozone over the United States in summer: Origin, trend, and contribution to pollution episodes, J. Geophys. Res., 107, 4275, doi:10.1029/2001JD000982, 2002.

Fishman, J., Solomon, S., and Crutzen, P. J.: Observational and theoretical evidence in support of a significant in situ photochemical source of tropospheric ozone, Tellus, 31, 432–446, 1979.

Forster, C., Cooper, O., Stohl, A., Eckhardt, S., James, P., Dunlea, E., Nicks, D. K., Holloway, J. S., Hubler, G., Parrish, D. D., Ryerson, T. B., and Trainer, M.: Lagrangian transport model forecasts and a transport climatology for the Intercontinental Transport and Chemical Transformation 2002 (ITCT 2K2) measurement campaign, J. Geophys. Res.-Atmos., 109, D07s92, doi:10.1029/2003JD003589, 2004.

Fuchs, H., Simpson, W. R., Apodaca, R. L., Brauers, T., Cohen, R. C., Crowley, J. N., Dorn, H.-P., Dubé, W. P., Fry, J. L., Häseler, R., Kajii, Y., Kiendler-Scharr, A., Labazan, I., Matsumoto, J., Mentel, T. F., Nakashima, Y., Rohrer, F., Rollins, A. W., Schuster, G., Tillmann, R., Wahner, A., Wooldridge, P. J., and Brown, S. S.: Comparison of N_2O_5 mixing ratios during NO3Comp 2007 in SAPHIR, Atmos. Meas. Tech., 5, 2763–2777, doi:10.5194/amt-5-2763-2012, 2012.

Heald, C. L., Jacob, D. J., Fiore, A. M., Emmons, L. K., Gille, J. C., Deeter, M. N., Warner, J., Edwards, D. P., Crawford, J. H., Hamlin, A. J., Sachse, G. W., Browell, E. V., Avery, M. A., Vay, S. A., Westberg, D. J., Blake, D. R., Singh, H. B., Sandholm, S. T., Talbot, R. W., and Fuelberg, H. E.: Asian outflow and trans-Pacific transport of carbon monoxide and ozone pollution: An integrated satellite, aircraft, and model perspective, J. Geophys. Res.-Atmos., 108, 4804, doi:10.1029/2003JD003507, 2003.

Hoell, J. M., Davis, D., Liu, S. C., Newell, R., Shipham, M., Akimoto, H., McNeal, R. J., Bendura, R. J., and Drewry, J. W.: Pacific Exploratory Mission-West A (PEM-West A): September October 1991, J. Geophys. Res.-Atmos., 101, 1641–1653, 1996.

Hoell, J. M., Davis, D. D., Liu, S. C., Newell, R. E., Akimoto, H., McNeal, R. J., and Bendura, R. J.: The Pacific Exploratory Mission - West phase B: February-March, 1994, J. Geophys. Res.-Atmos., 102, 28223–28239, 1997.

Holland, E. A., Braswell, B. H., Sulzman, J., and Lamarque, J. F.: Nitrogen deposition onto the United States and western Europe: Synthesis of observations and models, Ecol. Appl., 15, 38–57, doi:10.1890/03-5162, 2005.

Horowitz, L. W. and Jacob, D. J.: Global impact of fossil fuel combustion on atmospheric NO_x, J. Geophys. Res.-Atmos., 104, 23823–23840, 1999.

Hsu, N. C., Li, C., Krotkov, N. A., Liang, Q., Yang, K., and Tsay, S. C.: Rapid transpacific transport in autumn observed by the A-train satellites, J. Geophys. Res.-Atmos., 117, D06312, doi:10.1029/2011JD016626, 2012.

Hudman, R. C., Jacob, D. J., Cooper, O. R., Evans, M. J., Heald, C. L., Park, R. J., Fehsenfeld, F., Flocke, F., Holloway, J., Hubler, G., Kita, K., Koike, M., Kondo, Y., Neuman, A., Nowak, J., Oltmans, S., Parrish, D., Roberts, J. M., and Ryerson, T.: Ozone production in transpacific Asian pollution plumes and implications for ozone air quality in California, J. Geophys. Res., 109, D23s10, doi:10.1029/2004jd004974, 2004.

Jacob, D. J., Logan, J. A., and Murti, P. P.: Effect of rising Asian emissions on surface ozone in the United States, Geophys. Res. Lett., 26, 2175–2178, doi:10.1029/1999gl900450, 1999.

Jacob, D. J., Crawford, J. H., Kleb, M. M., Connors, V. S., Bendura, R. J., Raper, J. L., Sachse, G. W., Gille, J. C., Emmons, L., and Heald, C. L.: Transport and Chemical Evolution over the Pacific (TRACE-P) aircraft mission: Design, execution, and first results, J. Geophys. Res., 108, 1–19, 2003.

Jaffe, D., Anderson, T., Covert, D., Kotchenruther, R., Trost, B., Danielson, J., Simpson, W., Berntsen, T., Karlsdottir, S., Blake, D., Harris, J., Carmichael, G., and Uno, I.: Transport of Asian air pollution to North America, Geophys. Res. Lett., 26, 711–714, doi:10.1029/1999gl900100, 1999.

Jaffe, D., Anderson, T., Covert, D., Trost, B., Danielson, J., Simpson, W., Blake, D., Harris, J., and Streets, D.: Observations of ozone and related species in the northeast Pacific during the PHOBEA campaigns 1. Ground-based observations at Cheeka Peak, J. Geophys. Res.-Atmos., 106, 7449–7461, 2001.

Jaffe, D., Price, H., Parrish, D., Goldstein, A., and Harris, J.: Increasing background ozone during spring on the west coast of North America, Geophys. Res. Lett., 30, 1613, doi:10.1029/2003GL017024, 2003.

Jordan, C. E., Dibb, J. E., Anderson, B. E., and Fuelberg, H. E.: Uptake of nitrate and sulfate on dust aerosols during TRACE-P, J. Geophys. Res.-Atmos., 108, 1–10, doi:10.1029/2002JD003101, 2003.

Kirchner, F., Mayer-Figge, A., Zabel, F., and Becker, K. H.: Thermal stability of peroxynitrates, Int. J. Chem. Kinet., 31, 127–144, 1999.

Kirchner, W., Welter, F., Bongartz, A., Kames, J., Schweighoefer, S., and Schurath, U.: Trace Gas-Exchange at the Air-Water-Interface – Measurements of Mass Accommodation Coefficients, J. Atmos. Chem., 10, 427–449, 1990.

Kleb, M. M., Chen, G., Crawford, J. H., Flocke, F. M., and Brown, C. C.: An overview of measurement comparisons from the INTEX-B/MILAGRO airborne field campaign, Atmos. Meas. Tech., 4, 9–27, doi:10.5194/amt-4-9-2011, 2011.

Koike, M., Kondo, Y., Kawakami, S., Singh, H. B., Ziereis, H., and Merrill, J. T.: Ratios of reactive nitrogen species over the Pacific during PEM-West A, J. Geophys. Res.-Atmos., 101, 1829–1851, doi:10.1029/95JD02728, 1996.

Koike, M., Kondo, Y., Kita, K., Takegawa, N., Masui, Y., Miyazaki, Y., Ko, M. W., Weinheimer, A. J., Flocke, F., Weber, R. J., Thornton, D. C., Sachse, G. W., Vay, S. A., Blake, D. R., Streets, D. G., Eisele, F. L., Sandholm, S. T., Singh, H. B., and Talbot, R. W.: Export of anthropogenic reactive nitrogen and sulfur compounds from the East Asia region in spring, J. Geophys. Res.-Atmos., 108, 8789, doi:10.1029/2002JD003284, 2003.

Kotchenruther, R. A., Jaffe, D. A., Beine, H. J., Anderson, T. L., Bottenheim, J. W., Harris, J. M., Blake, D. R., and Schmitt, R.: Observations of Ozone and related species in the northeast Pacific during the PHOBEA campaigns 2.

Airborne observations, J. Geophys. Res.-Atmos., 106, 7463–7483, doi:10.1029/2000jd900425, 2001a.

Kotchenruther, R. A., Jaffe, D. A., and Jaegle, L.: Ozone photochemistry and the role of peroxyacetyl nitrate in the springtime northeastern Pacific troposphere: Results from the Photochemical Ozone Budget of the Eastern North Pacific Atmosphere (PHOBEA) campaign, J. Geophys. Res.-Atmos., 106, 28731–28742, doi:10.1029/2000JD000060, 2001c.

Lamarque, J. F., Brasseur, G. P., and Hess, P. G.: Three-dimensional study of the relative contributions of the different nitrogen sources in the troposphere, J. Geophys. Res.-Atmos., 101, 22955–22968, 1996.

Liu, H. Y., Jacob, D. J., Bey, I., Yantosca, R. M., Duncan, B. N., and Sachse, G. W.: Transport pathways for Asian pollution outflow over the Pacific: Interannual and seasonal variations, J. Geophys. Res.-Atmos., 108, 8786, doi:10.1029/2002JD003102, 2003.

McNaughton, C. S., Clarke, A. D., Kapustin, V., Shinozuka, Y., Howell, S. G., Anderson, B. E., Winstead, E., Dibb, J., Scheuer, E., Cohen, R. C., Wooldridge, P., Perring, A., Huey, L. G., Kim, S., Jimenez, J. L., Dunlea, E. J., DeCarlo, P. F., Wennberg, P. O., Crounse, J. D., Weinheimer, A. J., and Flocke, F.: Observations of heterogeneous reactions between Asian pollution and mineral dust over the Eastern North Pacific during INTEX-B, Atmos. Chem. Phys., 9, 8283–8308, doi:10.5194/acp-9-8283-2009, 2009.

Miyazaki, Y., Kondo, Y., Koike, M., Fuelberg, H. E., Kiley, C. M., Kita, K., Takegawa, N., Sachse, G. W., Flocke, F., Weinheimer, A. J., Singh, H. B., Eisele, F. L., Zondlo, M., Talbot, R. W., Sandholm, S. T., Avery, M. A., and Blake, D. R.: Synoptic-scale transport of reactive nitrogen over the western Pacific in spring, J. Geophys. Res., 108, 8788, doi:10.1029/2002JD003248, 2003.

Moxim, W. J., Levy, H., and Kasibhatla, P. S.: Simulated global tropospheric PAN: Its transport and impact on NO_x, J Geophys Res.-Atmos., 101, 12621–12638, 1996.

Munger, J. W., Wofsy, S. C., Bakwin, P. S., Fan, S. M., Goulden, M. L., Daube, B. C., Goldstein, A. H., Moore, K. E., and Fitzjarrald, D. R.: Atmospheric deposition of reactive nitrogen oxides and ozone in a temperate deciduous forest and a subarctic woodland .1. Measurements and mechanisms, J. Geophys. Res.-Atmos., 101, 12639–12657, 1996.

Munger, J. W., Fan, S. M., Bakwin, P. S., Goulden, M. L., Goldstein, A. H., Colman, A. S., and Wofsy, S. C.: Regional budgets for nitrogen oxides from continental sources: Variations of rates for oxidation and deposition with season and distance from source regions, J. Geophys. Res.-Atmos., 103, 8355–8368, 1998.

Nowak, J. B., Parrish, D. D., Neuman, J. A., Holloway, J. S., Cooper, O. R., Ryerson, T. B., Nicks, D. K., Flocke, F., Roberts, J. M., Atlas, E., de Gouw, J. A., Donnelly, S., Dunlea, E., Hubler, G., Huey, L. G., Schauffler, S., Tanner, D. J., Warneke, C., and Fehsenfeld, F. C.: Gas-phase chemical characteristics of Asian emission plumes observed during ITCT 2K2 over the eastern North Pacific Ocean, J. Geophys. Res.-Atmos., 109, D23s19, doi:10.1029/2003JD004488, 2004.

Noxon, J. F., Norton, R. B., and Henderson, W. R.: Observation of atmospheric NO_3, Geophys. Res. Lett., 5, 675–678, 1978.

Parrish, D. D., Hahn, C. J., Williams, E. J., Norton, R. B., Fehsenfeld, F. C., Singh, H. B., Shetter, J. D., Gandrud, B. W., and Ridley, B. A.: Indications of Photochemical Histories of Pacific Air Masses from Measurements of Atmospheric Trace Species at Point Arena, California, J. Geophys. Res.-Atmos., 97, 15883–15901, 1992.

Parrish, D. D., Dunlea, E. J., Atlas, E. L., Schauffler, S., Donnelly, S., Stroud, V., Goldstein, A. H., Millet, D. B., McKay, M., Jaffe, D. A., Price, H. U., Hess, P. G., Flocke, F., and Roberts, J. M.: Changes in the photochemical environment of the temperate North Pacific troposphere in response to increased Asian emissions, J. Geophys. Res.-Atmos., 109, D23s18, doi:10.1029/2004GL004978, 2004a.

Parrish, D. D., Kondo, Y., Cooper, O. R., Brock, C. A., Jaffe, D. A., Trainer, M., Ogawa, T., Hubler, G., and Fehsenfeld, F. C.: Intercontinental Transport and Chemical Transformation 2002 (ITCT 2K2) and Pacific Exploration of Asian Continental Emission (PEACE) experiments: An overview of the 2002 winter and spring intensives, J. Geophys. Res., 109, D23s01, doi:10.1029/2004jd004980, 2004b.

Parrish, D. D., Millet, D. B., and Goldstein, A. H.: Increasing ozone in marine boundary layer inflow at the west coasts of North America and Europe, Atmos. Chem. Phys., 9, 1303–1323, doi:10.5194/acp-9-1303-2009, 2009.

Perring, A. E., Bertram, T. H., Farmer, D. K., Wooldridge, P. J., Dibb, J., Blake, N. J., Blake, D. R., Singh, H. B., Fuelberg, H., Diskin, G., Sachse, G., and Cohen, R. C.: The production and persistence of $\Sigma RONO_2$ in the Mexico City plume, Atmos. Chem. Phys., 10, 7215–7229, doi:10.5194/acp-10-7215-2010, 2010.

Platt, U., Perner, D., Winer, A. M., Harris, G. W., and Pitts, J. N.: Detection of NO_3 in the polluted troposphere by differential optical-absorption, Geophys. Res. Lett., 7, 89–92, 1980.

Pusede, S. E. and Cohen, R. C.: On the observed response of ozone to NO_x and VOC reactivity reductions in San Joaquin Valley California 1995–present, Atmos. Chem. Phys., 12, 8323–8339, doi:10.5194/acp-12-8323-2012, 2012.

Richter, A., Burrows, J. P., Nuss, H., Granier, C., and Niemeier, U.: Increase in tropospheric nitrogen dioxide over China observed from space, Nature, 437, 129–132, doi:10.1038/Nature04092, 2005.

Roberts, J. M., Flocke, F., Chen, G., de Gouw, J., Holloway, J. S., Hubler, G., Neuman, J. A., Nicks, D. K., Nowak, J. B., Parrish, D. D., Ryerson, T. B., Sueper, D. T., Warneke, C., and Fehsenfeld, F. C.: Measurement of peroxycarboxylic nitric anhydrides (PANs) during the ITCT 2K2 aircraft intensive experiment, J. Geophys. Res., 109, D23s21, doi:10.1029/2004jd004960, 2004.

Rollins, A. W., Browne, E. C., Min, K. E., Pusede, S. E., Wooldridge, P. J., Gentner, D. R., Goldstein, A. H., Liu, S., Day, D. A., Russell, L. M., and Cohen, R. C.: Evidence for NO_x Control over Nighttime SOA Formation, Science, 337, 1210–1212, doi:10.1126/science.1221520, 2012.

Sander, R.: Compilation of Henry's Law Constants for Inorganic and Organic Species of Potential Importance in Environmental Chemistry (Version 3) Rep., Mainz, Germany, 1999.

Singh, H. B., Salas, L. J., Ridley, B. A., Shetter, J. D., Donahue, N. M., Fehsenfeld, F. C., Fahey, D. W., Parrish, D. D., Williams, E. J., Liu, S. C., Hubler, G., and Murphy, P. C.: Relationship between Peroxyacetyl Nitrate and Nitrogen-Oxides in the Clean Troposphere, Nature, 318, 347–349, 1985.

Singh, H. B., Salas, L. J., and Viezee, W.: Global Distribution of Peroxyacetyl Nitrate, Nature, 321, 588–591, 1986.

Singh, H. B., Herlth, D., Kolyer, R., Salas, L., Bradshaw, J. D., Sandholm, S. T., Davis, D. D., Crawford, J., Kondo, Y., Koike, M., Talbot, R., Gregory, G. L., Sachse, G. W., Browell, E., Blake, D. R., Rowland, F. S., Newell, R., Merrill, J., Heikes, B., Liu, S. C., Crutzen, P. J., and Kanakidou, M.: Reactive nitrogen and ozone over the western Pacific: Distribution, partitioning, and sources, J. Geophys. Res.-Atmos., 101, 1793–1808, doi:10.1029/95JD01029, 1996.

Singh, H. B., Viezee, W., Chen, Y., Thakur, A. N., Kondo, Y., Talbot, R. W., Gregory, G. L., Sachse, G. W., Blake, D. R., Bradshaw, J. D., Wang, Y., and Jacob, D. J.: Latitudinal distribution of reactive nitrogen in the free troposphere over the Pacific Ocean in late winter early spring, J. Geophys. Res., 103, 28237–28246, 1998.

Stohl, A.: A 1-year Lagrangian "climatology" of airstreams in the Northern Hemisphere troposphere and lowermost stratosphere, J. Geophys. Res.-Atmos., 106, 7263–7279, 2001.

Streets, D. G., Bond, T. C., Carmichael, G. R., Fernandes, S. D., Fu, Q., He, D., Klimont, Z., Nelson, S. M., Tsai, N. Y., Wang, M. Q., Woo, J. H., and Yarber, K. F.: An inventory of gaseous and primary aerosol emissions in Asia in the year 2000, J. Geophys. Res.-Atmos., 108, 8809, doi:10.1029/2002JD003093, 2003.

Talbot, R. W., Dibb, J. E., Lefer, B. L., Scheuer, E. M., Bradshaw, J. D., Sandholm, S. T., Smyth, S., Blake, D. R., Blake, N. J., Sachse, G. W., Collins, J. E., and Gregory, G. L.: Large-scale distributions of tropospheric nitric, formic, and acetic acids over the western Pacific basin during wintertime, J. Geophys. Res.-Atmos., 102, 28303–28313, 1997.

Talbot, R., Dibb, J., Scheuer, E., Seid, G., Russo, R., Sandholm, S., Tan, D., Singh, H., Blake, D., Blake, N., Atlas, E., Sachse, G., Jordan, C., and Avery, M.: Reactive nitrogen in Asian continental outflow over the western Pacific: Results from the NASA Transport and Chemical Evolution over the Pacific (TRACE-P) airborne mission, J. Geophys. Res.-Atmos., 108, 8803, doi:10.1029/2002jd003129, doi:10.1029/2002JD003129, 2003.

Talukdar, R. K., Burkholder, J. B., Schmoltner, A. M., Roberts, J. M., Wilson, R. R., and Ravishankara, A. R.: Investigation of the Loss Processes for Peroxyacetyl Nitrate in the Atmosphere – Uv Photolysis and Reaction with Oh, J. Geophys. Res. Atmos., 100, 14163–14173, 1995.

Tang, M. J., Thieser, J., Schuster, G., and Crowley, J. N.: Uptake of NO_3 and $N_2O{-}5$ to Saharan dust, ambient urban aerosol and soot: a relative rate study, Atmos. Chem. Phys., 10, 2965–2974, doi:10.5194/acp-10-2965-2010, 2010.

Thaler, R. D., Mielke, L. H., and Osthoff, H. D.: Quantification of Nitryl Chloride at Part Per Trillion Mixing Ratios by Thermal Dissociation Cavity Ring-Down Spectroscopy, Anal. Chem., 83, 2761–2766, doi:10.1021/AC200055Z, 2011.

Thornton, J. A., Wooldridge, P. J., and Cohen, R. C.: Atmospheric NO_2: In situ laser-induced fluorescence detection at parts per trillion mixing ratios, Anal. Chem., 72, 528–539, 2000.

Thornton, J. A., Wooldridge, P. J., Cohen, R. C., Martinez, M., Harder, H., Brune, W. H., Williams, E. J., Roberts, J. M., Fehsenfeld, F. C., Hall, S. R., Shetter, R. E., Wert, B. P., and Fried, A.: Ozone production rates as a function of NO_x abundances and HO_x production rates in the Nashville urban plume, J. Geophys. Res., 107, 4146, doi:10.1029/2001jd000932, 2002.

Tolocka, M. P., Saul, T. D., and Johnston, M. V.: Determination of nitric acid uptake onto sodium chloride particles, Abstracts of Papers of the American Chemical Society, 224, U347–U347, 2002.

Trainer, M., Buhr, M. P., Curran, C. M., Fehsenfeld, F. C., Hsie, E. Y., Liu, S. C., Norton, R. B., Parrish, D. D., Williams, E. J., Gandrud, B. W., Ridley, B. A., Shetter, J. D., Allwine, E. J., and Westberg, H. H.: Observations and Modeling of the Reactive Nitrogen Photochemistry at a Rural Site, J. Geophys. Res.-Atmos., 96, 3045–3063, 1991.

Turnipseed, A. A., Huey, L. G., Nemitz, E., Stickel, R., Higgs, J., Tanner, D. J., Slusher, D. L., Sparks, J. P., Flocke, F., and Guenther, A.: Eddy covariance fluxes of peroxyacetyl nitrates (PANs) and NO_y to a coniferous forest, J. Geophys. Res., 111, D09304, doi:10.1029/2005JD006631, 2006.

Walker, T. W., Martin, R. V., van Donkelaar, A., Leaitch, W. R., MacDonald, A. M., Anlauf, K. G., Cohen, R. C., Bertram, T. H., Huey, L. G., Avery, M. A., Weinheimer, A. J., Flocke, F. M., Tarasick, D. W., Thompson, A. M., Streets, D. G., and Liu, X.: Trans-Pacific transport of reactive nitrogen and ozone to Canada during spring, Atmos. Chem. Phys., 10, 8353–8372, doi:10.5194/acp-10-8353-2010, 2010.

Wolfe, G. M., Thornton, J. A., Yatavelli, R. L. N., McKay, M., Goldstein, A. H., LaFranchi, B., Min, K.-E., and Cohen, R. C.: Eddy covariance fluxes of acyl peroxy nitrates (PAN, PPN and MPAN) above a Ponderosa pine forest, Atmos. Chem. Phys., 9, 615–634, doi:10.5194/acp-9-615-2009, 2009.

Wooldridge, P. J., Perring, A. E., Bertram, T. H., Flocke, F. M., Roberts, J. M., Singh, H. B., Huey, L. G., Thornton, J. A., Wolfe, G. M., Murphy, J. G., Fry, J. L., Rollins, A. W., LaFranchi, B. W., and Cohen, R. C.: Total Peroxy Nitrates (SPNs) in the atmosphere: the Thermal Dissociation-Laser Induced Fluorescence (TD-LIF) technique and comparisons to speciated PAN measurements, Atmos. Meas. Tech., 3, 593–607, doi:10.5194/amt-3-593-2010, 2010.

Yienger, J. J., Galanter, M., Holloway, T. A., Phadnis, M. J., Guttikunda, S. K., Carmichael, G. R., Moxim, W. J., and Levy, H.: The episodic nature of air pollution transport from Asia to North America, J. Geophys. Res., 105, 26931–26945, 2000.

Zhang, L., Jacob, D. J., Boersma, K. F., Jaffe, D. A., Olson, J. R., Bowman, K. W., Worden, J. R., Thompson, A. M., Avery, M. A., Cohen, R. C., Dibb, J. E., Flock, F. M., Fuelberg, H. E., Huey, L. G., McMillan, W. W., Singh, H. B., and Weinheimer, A. J.: Transpacific transport of ozone pollution and the effect of recent Asian emission increases on air quality in North America: an integrated analysis using satellite, aircraft, ozonesonde, and surface observations, Atmos. Chem. Phys., 8, 6117–6136, doi:10.5194/acp-8-6117-2008, 2008.

Zhang, Q., Streets, D. G., He, K., Wang, Y., Richter, A., Burrows, J. P., Uno, I., Jang, C. J., Chen, D., Yao, Z., and Lei, Y.: NO_x emission trends for China, 1995–2004: The view from the ground and the view from space, J. Geophys. Res.-Atmos., 112, D09304, doi:10.1029/2007JD008684, 2007.

Zhang, Q., Streets, D. G., Carmichael, G. R., He, K. B., Huo, H., Kannari, A., Klimont, Z., Park, I. S., Reddy, S., Fu, J. S., Chen, D., Duan, L., Lei, Y., Wang, L. T., and Yao, Z. L.: Asian emissions in 2006 for the NASA INTEX-B mission, Atmos. Chem. Phys., 9, 5131–5153, doi:10.5194/acp-9-5131-2009, 2009.